

Magnetoresistance of icosahedral Al-Pd-Re: From weak localization through breakdown to a high-resistivity regime

M. Rodmar, M. Ahlgren, and D. Oberschmidt

Department of Solid State Physics, Kungliga Tekniska Högskolan, SE 10044 Stockholm, Sweden

C. Gignoux, J. Delahaye, and C. Berger

Laboratoire d'Études des Propriétés Électroniques, CNRS, Boîte Postale 166, 38042 Grenoble Cedex 9, France

S. J. Poon

Department of Physics, University of Charlottesville, Charlottesville, Virginia 22901

Ö. Rapp

Department of Solid State Physics, Kungliga Tekniska Högskolan, SE 10044 Stockholm, Sweden

(Received 1 February 1999; revised manuscript received 2 November 1999)

The magnetoresistance (MR) of icosahedral Al-Pd-Re of nominal composition $\text{Al}_{70.5}\text{Pd}_{21}\text{Re}_{8.5}$, and with resistance ratios $R [= \rho(4 \text{ K})/\rho(295 \text{ K})]$ from 2 to 120, has been measured in the range 0.1–40 K in magnetic fields up to 12 T. Three regions of the MR can be distinguished. For R up to 13 quantum interference effects (QIE) describe the observations well. MR in excess of 100% was observed at low temperatures in this region. For R increasing above 13, the approach of a possible metal-insulator transition (MIT) can be followed in the results. A new negative MR contribution emerges at the lowest temperature, 0.2 K, and increases in magnitude with R . From analyses within QIE the Coulomb interaction parameter above $R \approx 10$ and the inelastic-scattering time decrease with R , and the results indicate that this may be the case also for the spin-orbit-scattering rate. For $R \geq 50$, weak localization has broken down. Samples prepared by two different methods were studied in this region of R . Although the temperature dependence of the electrical resistivity and the MR at temperatures above 4 K are similar for similar R values in both sets of samples, significant differences were observed below 1 K. We discuss this MR in the light of current theories on both sides of an MIT and conclude that none of these theories can fully reproduce the observed features for samples in this range.

I. INTRODUCTION

Electronic transport in all stable icosahedral quasicrystals is characterized by unusual properties such as a large resistivity ρ , a strong temperature dependence of ρ , in general an increase in ρ for improved atomic ordering, a large magnetoresistance, and sign reversals in the thermopower and Hall constant as a function of temperature or ρ . The magnetoresistance is unique among these anomalies. Only in this area a large part of the observations can be understood within an established theoretical framework, in this case quantum interference effects (QIE),¹ i.e., corrections to the Boltzmann conductivity that arise from the diffusive motion of intensely scattered electrons. In some cases QIE can describe these observations over a larger temperature range and with much better quantitative precision than previously found in other three-dimensional alloys.² The electrons thus behave as in a disordered system, in spite of the long-range atomic ordering, of coherence lengths in excess of $1 \mu\text{m}$.³

An exception to such a description in terms of QIE is high-resistivity icosahedral (*i*)-Al-Pd-Re. In this case, the magnetoresistance (MR) is inconsistent with weak localization and electron-electron interactions, with a negative MR at low temperatures and for low-magnetic fields, which changes sign with increasing field to positive values.^{4–6} In contrast, for samples of smaller resistivities such as some

pure *i*-Al-Pd-Re alloys,^{7–10} and Mn,¹¹ and Ru¹² doped samples, the MR can be described by QIE. Hence, there should be a breakdown at an intermediate value of the resistivity. However, the analyses of Refs 9–12 were limited to at most a few samples in the weakly metallic regime. Our Refs. 7 and 8 were brief conference reports. Therefore, details on how this transition occurs have not been obtained.

Beyond the weakly metallic regime the resistivity can reach values of $\rho(4 \text{ K}) > 1 \Omega \text{ cm}$ with resistance ratios $R [= \rho(4.2 \text{ K})/\rho(295 \text{ K})]$ in a range of values up to 100,^{4,13,14} or even 200,⁶ and above,¹⁵ suggesting the possibility of a metal-insulator transition (MIT). Analyses of $\rho(T)$ in terms of variable range hopping^{11,16} (VRH) have indicated an insulating state. However, other results suggest a saturation of the resistivity at low temperatures,¹⁷ less than 1 K. This question remains unresolved, and the nature of a possible MIT is not understood.

For the magnetoresistance of high resistivity *i*-Al-Pd-Re the situation is even less clear. From the theoretical point of view there is no agreement on the MR on the insulating side of an MIT. Several contrasting theories will be described below. Nor is there any clear picture of the experimental situation, and the published results on the MR of *i*-Al-Pd-Re in this resistivity region are difficult to compare.^{4,6,7,9–12,18} These samples were prepared by different techniques such as melt spinning,^{4,6,7,18} samples cut from ingots prepared in an

arcfurnace,^{9,11} and pulling of arc-melted ingots into bars.^{10,12} Various heat treatments have then been applied. These differences affect sample morphology and sample properties, but it is not known in detail how. In most of the quoted papers, the break down of QIE was illustrated by one or two samples with R values spanning the large range from from⁹ 7 to¹⁸ 190, and sample properties were correspondingly different. Furthermore, the relation between $\rho(4\text{ K})$ and R varies between some of these reports, which further complicates overview.

In the present paper we aim at a comprehensive study of the MR of i -Al-Pd-Re over the full range of its varying behavior. Samples with resistance ratios R from 2 to 120 are studied, roughly corresponding to $\rho(4\text{ K})$ in the range 6–1000 m Ω cm. This subject is conveniently divided into three parts. After a description of experimental details in Sec. II, samples of low R in the region of conventional QIE are discussed in Sec. III, including experimental results, analysis methods, and results of the analyses. At larger R and ρ values, the extraction of information from QIE becomes increasingly difficult. Section IV describes how analyses in variable temperature regions can be used to obtain information on the inelastic-scattering time and other parameters in the vicinity of breakdown of QIE. The high- ρ alloys are discussed in Sec. V. In order to address to some extent this unclear situation, two series of differently prepared samples are studied and compared. Section VI is a brief summary.

II. DETAILS OF SAMPLES AND EXPERIMENTS

A. Sample preparation

Sample of the nominal composition Al_{70.5}Pd₂₁Re_{8.5} were made with one of the two following preparation methods. Some further details of the preparation techniques have been given previously.^{19,20}

Method A. Samples were melted in an arc furnace and subsequently annealed at 940 and 600–650 °C. The ingot was then quenched in water. Samples of a typical size of $1 \times 1 \times 5\text{ mm}^3$ were cut from the ingot.

Method B. The constituents were melted in appropriate amounts in an arc furnace. The ingots were melt spun and thereafter annealed in varying cycles in the temperature range 800–1000 °C. The ribbons were finally slowly cooled in the furnace. Sample thickness was typically 30 μm .

Resistance ratios can be easily measured in contrast to the resistivity and are almost linearly correlated with ρ as noted previously for B samples.¹⁹ As described below, this relation is valid also for A samples provided a correction for their morphology is made. R can therefore conveniently be used as a sample-characterizing parameter for all samples.

For the range of intermediate resistivity, Secs. III and IV, six B samples were studied with R values of 2, 4, 11, 13, 23, and 45. In Sec. V samples in a range of larger R values from about 50–120 were investigated for both A and B samples.

B. Sample characterization

Standard powder-x-ray diffraction on crushed Al-Pd-Re ribbons from the same batches could be indexed with the single icosahedral phase. It should be noted that the patterns were obtained from ribbons of different R 's. The narrow

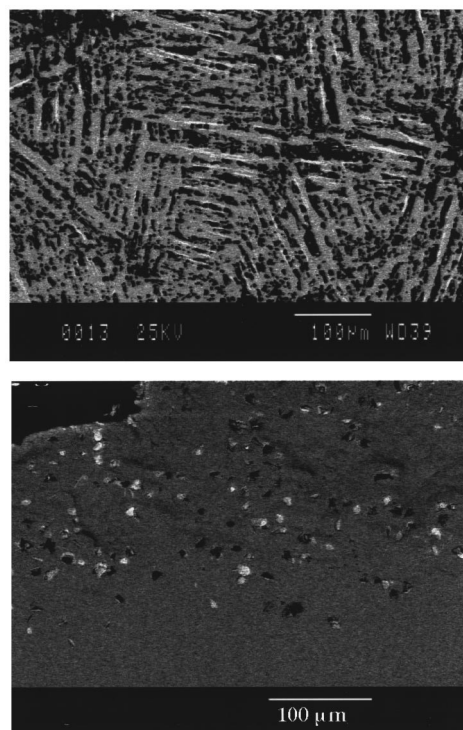


FIG. 1. SEM picture (backscattered electrons) of an A sample with $R=85$ (top panel) and a B sample with $R=119$ (bottom panel). The gray areas consist of the icosahedral phase, the white areas of secondary phase, and the black areas are the voids. The observed secondary phase and the voids on the B sample are observable only close to the surface.

peaks have widths within the experimental resolution, which is a good indication of the structural quality of the samples.

For low- R samples, scanning electron microscopy (SEM) and microprobe analysis on typical ribbons reveal that some samples may contain secondary phases, the presence of which is not correlated to the R value.²¹ The magnetoresistance, to be discussed below, gives further evidence that the measured transport properties are due to the icosahedral phase.

Some high- R samples have been studied in SEM. In Fig. 1 pictures of an A and B sample are shown in the top and bottom panels, respectively. The A samples had voids in the shape of needles, roughly of 30% volume fraction and of length about 100–400 μm . The samples had a secondary phase mainly consisting of Al and Re. The B samples were homogenous and had no voids. There were, however, some secondary phase (about 5%) on the surface of the ribbons. The secondary phase in the B samples also seemed mainly to consist of Al and Re, but the Al content was higher than in the secondary phase in the A samples. In Fig. 1 the icosahedral phase is gray, voids are black, and the secondary phase is seen as white areas.

The irregular morphology of the A samples results in an overestimation of their resistivity if the geometrical form factors are used without any compensation for voids. The actual conductivity of A samples was recently calculated in a model considering the voids to be needle shaped and imbedded in a single-phase macroscopically isotropic material.¹⁷ It was then found that the relation between R and the so determined $\rho(4\text{ K})$ of the A samples was similar to that of the B samples.

C. Measurement techniques

Electrical contacts were made with silver paint. The contact resistances of order 1 Ω were comparable to the sample resistances at room temperature. Standard dc measurements were made with a four-probe technique and low-current densities. Below 1 K, a dilution refrigerator was used, equipped with superconducting solenoid to 6 T. Measurements above 1.5 K were performed in a flowing-gas cryostat with a 12-T superconducting coil. The low-temperature measurements were made with a small dc current, of about nA, in order to prevent any heating effects of the samples. The measurement current was adjusted to insure that there was no heating effects. The voltage was measured with an EM Electronics picovoltmeter.

For samples with strongly temperature-dependent resistivity, such as *i*-Al-Pd-Re discussed here, temperature stabilization in magnetic field is usually a major experimental concern. Slightly different measurement procedures were used for the samples of intermediate *R* values in Secs. III and IV, and those of high-*R* values in Sec. V. In the former case, the measurements in a He⁴ cryostat were limited to 4.2 and 1.5 K, the pumping limit of the cryostat, which provided stable measurement temperatures. Below 1 K the problem of temperature stabilization is less serious both since $\rho(T)$ of these intermediate resistivity *i*-Al-Pd-Re was found to be considerably less temperature dependent,¹⁹ and also since the thermometers in this region either have a negligible magnetoresistance (a Ge-based sensor) or a small enough magnetoresistance (a carbon sensor) that it could be compensated for in a simple data program. Temperature errors are therefore believed to be negligible in these measurements.

For samples with large *R* and ρ , it was difficult to stabilize the temperature below 1 K during the long-magnetic-field sweeps necessary in order to prevent heating of the sample holder. The magnetoresistance measurements in this region were therefore performed with temperature sweeps at different constant fields. At temperatures above 1.5 K, an improved temperature regulation allowed measurements up to 40 K in field sweeps from 0–12–0 T with a temperature drift below a few mK.

III. QIE REGIME

The results for samples of intermediate resistivities are described and analyzed in terms of conventional quantum interference theories. We discuss in Sec. III A methods for analyses of QIE, in Sec. III B the results of the measurements, and in Sec. III C the analyses results.

A. Analyses methods

The two main contributions from quantum interference effects in nonsuperconducting materials are weak localization (WL) and electron-electron interactions (EEI) in the diffusion channel. The contributions to the magnetoconductivity $\Delta\sigma(B, T) = \sigma(B, T) - \sigma(0, T)$ from these effects^{22,23} can be schematically summarized as

$$\Delta\sigma_{\text{WL}} = \Delta\sigma[\tau_{\text{ic}}(T), \tau_{\text{so}}, D, g^*, B], \quad (1)$$

$$\Delta\sigma_{\text{EEI}} = \Delta\sigma(F_\sigma, D, g^*, B, T), \quad (2)$$

where $\tau_{\text{ic}}(T)$ is the inelastic-scattering time, τ_{so} the spin-orbit scattering time, D the diffusion coefficient, g^* the Landé factor, and F_σ the Coulomb interaction parameter.

The strong temperature dependence of $\sigma(T)$ in many quasicrystals gives rise to particular concerns when applying QIE to the magnetoresistance. Equations (1) and (2) should be calculated as corrections $\Delta\sigma$ to the background conductivity σ_0 , unaffected by QIE ($\sigma = \sigma_0 + \Delta\sigma_{\text{WL}} + \Delta\sigma_{\text{EEI}}$), but σ_0 is poorly known. In a method discussed previously² to handle this difficulty, two extremes were considered; (I) the (Boltzmann) background conductivity is assumed to be attained at 295 K, or (II) $\sigma_0 = \sigma(4 \text{ K})$, implying that QIE are not observed above 4 K. Assumption (II) is likely not well founded. Since QIE are observed in the magnetoresistance up to high temperatures, QIE presumably contribute to $\sigma(T)$ as well, although this is more difficult to unambiguously verify. Preference is thus given to method (I). However, we used both methods as a consistency check. When common trends were found in the two analyses for the parameters of QIE, this result is expected to be valid also for σ_0 evaluated at intermediate temperatures, thus greatly reducing the uncertainty introduced by the unknown σ_0 .

These considerations are important for the calculation of D . This is often a crucial parameter, since the calculated magnetoresistance is quite sensitive to the actual value, particularly for low- D materials. We assumed that the density of states $N(\epsilon_F)$ could be obtained from the electronic specific-heat coefficient γ , and calculated D from $D = [e^2 \rho N(\epsilon_F)]^{-1}$. The sensitivity of the resulting analyses to input values of ρ and γ must therefore be examined. The handling of these two parameters is now discussed.

Two methods were used to estimate ρ in analysis method (I): (a) an average room temperature ρ value of 3.5 m Ω cm was used for all samples, or (b) the measured ρ for each sample, in the range 2.5–4.5 m Ω cm, was used. Since the measurement error in ρ is about $\pm 20\%$ a weak trend of increase in $\rho(295 \text{ K})$ with *R* is barely discerned in these data. The results will be described below. A third way to handle ρ , avoiding the influence of random errors in this parameter, is to use ρ as an adjustable parameter. This method was examined for $R \leq 11$ in method (II), with results for $\rho(4 \text{ K})$ within experimental accuracy of the measured values.⁸ We have not further pursued this method, however, since it is roughly equivalent to multiplying the magnitude of the calculated QIE by an adjustable factor, and a breakdown of QIE could then be concealed.

Published results for γ of *i*-Al-Pd-Re vary between²⁴ 0.3 and²⁵ 0.1 mJ/mole K². There is a tendency for a decrease of γ with increasing ρ , in agreement with the empirical result that $\gamma \sim \rho(295 \text{ K})^{-1/2}$ for a large number of different icosahedral quasicrystals.^{1,26} In addition, two further circumstances complicate this problem. First, the conversion from γ to $N(\epsilon_F)$ is not straightforward. Two level tunneling states have been inferred from thermal-conductivity measurements and sound-velocity measurements,²⁷ and could also contribute to the specific heat with a term possibly linear in T . How to separate the measured γ into electronic and tunneling parts is not known. Furthermore, contributions to the specific heat of other forms might have to be considered. In *i*-Al-Cu-Fe, e.g., a sublinear T dependence of the specific heat has been observed below 1 K, and was ascribed to peculiarities of the

TABLE I. Notations of analyses with different D values. Some of these different analyses were also performed with $\gamma=0.14$ and/or 0.20 mJ/mole K^2 .

Notation	Background σ_0 (to which QIE are added)	$D=D(\rho, \gamma)$ γ usually 0.17 mJ/mole K^2
Method (Ia)	$\sigma(295 \text{ K})$	ρ = average $\rho_{295 \text{ K}}$ for all samples
(Ib)	$\sigma(295 \text{ K})$	ρ = meas. $\rho_{295 \text{ K}}$ for each sample
Method II	$\sigma(4.2 \text{ K})$	$\rho = \rho(4.2 \text{ K})$

vibrational states in quasicrystals or to the occurrence of localized spins.²⁸ Recently, similar results have been obtained in an i -Al-Pd-Re sample with $R \approx 80$, above the present range.²⁹

Due to these uncertainties in results for γ , and to the small variation of $\rho(295 \text{ K})$ for our samples, a constant γ was chosen as most appropriate and we used $\gamma = 0.17$ mJ/mole K^2 for all samples. To check on the sensitivity of the results to this assumption, some calculations were performed with $\gamma=0.14$ and 0.20 mJ/mole K^2 . The latter value was used previously³⁰ for an i -Al-Pd-Re sample with $R=4$, corresponding to the lower range of R values in the present samples.

The substantial errors in γ and ρ do not severely affect the conclusions of the analyses. We will be mostly interested in trends of the derived properties, which to first order are not sensitive to variations in the magnitude of the property derived. Furthermore, a factor of two difference in γ would appear to be a generous estimate of the error in this quantity, while the two methods of analyses, (I) and (II), lead to differences between D values by a factor in the range 2–23, and thus represent a much more acid test.

For convenient reference to the different methods used to calculate D , the notations are summarized in Table I. To reduce the number of freely varying parameters in the analyses and improve convergence, we assumed $g^*=2$, and used the measured ρ both for estimating D as discussed above, and for calculating $\Delta\sigma(B, T) = -\Delta\rho(B, T)/[\rho(0, T)\rho(B, T)]$ from the observations. $\tau_{ic}(T)$, τ_{so} , and F_σ were fitted to the data. $\tau_{ic}(T)$ was allowed to vary freely at each temperature, sometimes with the additional, physically reasonable constraint that $\tau_{ic}(T)$ cannot increase with increasing temperature, while τ_{so} and F_σ were taken to be constants for each sample.

B. Experimental results

Results for R , $\rho(4 \text{ K})$, and $\rho(1.5 \text{ K})$ are listed in Table II for the six samples studied in this Section and Sec. IV. The magnetoresistance is shown for five samples in Figs. 2(a)–

TABLE II. Resistance ratio R and ρ at two temperatures for the six i -Al_{70.5}Pd₂₁Re_{8.5} samples. An estimated error of the measurements of $\rho(295 \text{ K})$ is $\pm 20\%$. $R = \rho(4.2 \text{ K})/\rho(295 \text{ K})$.

R	2	4	11	13	23	45
$\rho(4.2 \text{ K})$ (m Ω cm)	6.1	17	29	45	88	210
$\rho(1.5 \text{ K})$ (m Ω cm)	6.2	18	39	65	140	460

2(e) as $\Delta\rho(B, T)/\rho(0, T)$ vs B at different temperatures from 0.2 to 4.2 K, and in Fig. 2(f) for a sample with $R=45$ at 4.2 K. Curves are fits to quantum interference effects and will be described below.

The results indicate that the observed magnetoresistance is due to the icosahedral phase, with no significant contribution from possible metallic impurities. Various two phase models for the conductivity have been attempted, but were discarded since we could not account for the observed magnetoresistance by any impurity phase at the level consistent with the x-ray-diffraction results. Furthermore, the magnetoresistance at 1.5 K and high fields increases by a factor of 3 in each step when going from $R=2$, to 4 and to 11, (Fig. 3). It would seem quite unpalatable with an increased importance of an impurity phase of unknown properties accounting for these observations.

A first striking feature of the results in Fig. 2 is the change of the shape of the magnetoresistance occurring when R increases from 23 to 45. For $R \leq 23$, one can notice that $\Delta\rho(B, T)/\rho(0, T)$ at low temperatures has a form close to $B^{1/2}$, while at 4.2 K a transition takes place, with increasing R towards a larger magnetic-field region with $\Delta\rho(B, T)/\rho(0, T) \sim B^2$. This is consistent with EEI and WL in strong spin-orbit scattering systems, where $\Delta\rho(B, T)/\rho(0, T)$ increases as B^2 at low fields and as $B^{1/2}$ at intermediate fields and the field strength is approximately measured by B/T . For $R=45$, the result is qualitatively similar to previous reports for high ρ samples,^{4–6} with an initial negative magnetoresistance and a sign change to positive values above 5 T at 4.2 K for this sample.

A second striking feature in Fig. 2 is the large magnetoresistance, in excess of 100%, which is observed at low temperatures for samples with R in the range 11–13. Such large values are unique in metalliclike alloys, and similar in magnitude to observations across the metal-insulator transition in metal-oxide or semiconducting-oxide systems.^{31,32}

Figure 2 shows that $\Delta\rho(B, T)/\rho(0, T)$ increases strongly with R at all temperatures up to an R value in the range 13–23. This is illustrated at 1.5 K in Fig. 3 for a few magnetic fields. From QIE theories it is expected that $\Delta\rho(B, T)/\rho(0, T)$ grows with ρ as $\sim \rho^\beta$, where β is a factor of order 1.5, and empirically found¹ to be ≈ 1.3 when data for systems with large MR are included.³³ Thus $|\Delta\sigma(B, T)|$ increases weakly with ρ . This point is illustrated in Fig. 4, where $-\Delta\sigma(B, 1.5 \text{ K})$ vs B is shown for the samples with $R=2$ and 11. The curves are decomposed fits to QIE described below. $-\Delta\sigma$ is about 1.5 times larger at $R=11$ than at $R=2$ for $B \leq 10$ T below saturation for the $R=11$ sample, which is roughly equal to the corresponding resistance ratio from Table II to the power 0.3 (≈ 1.7). This order of magni-

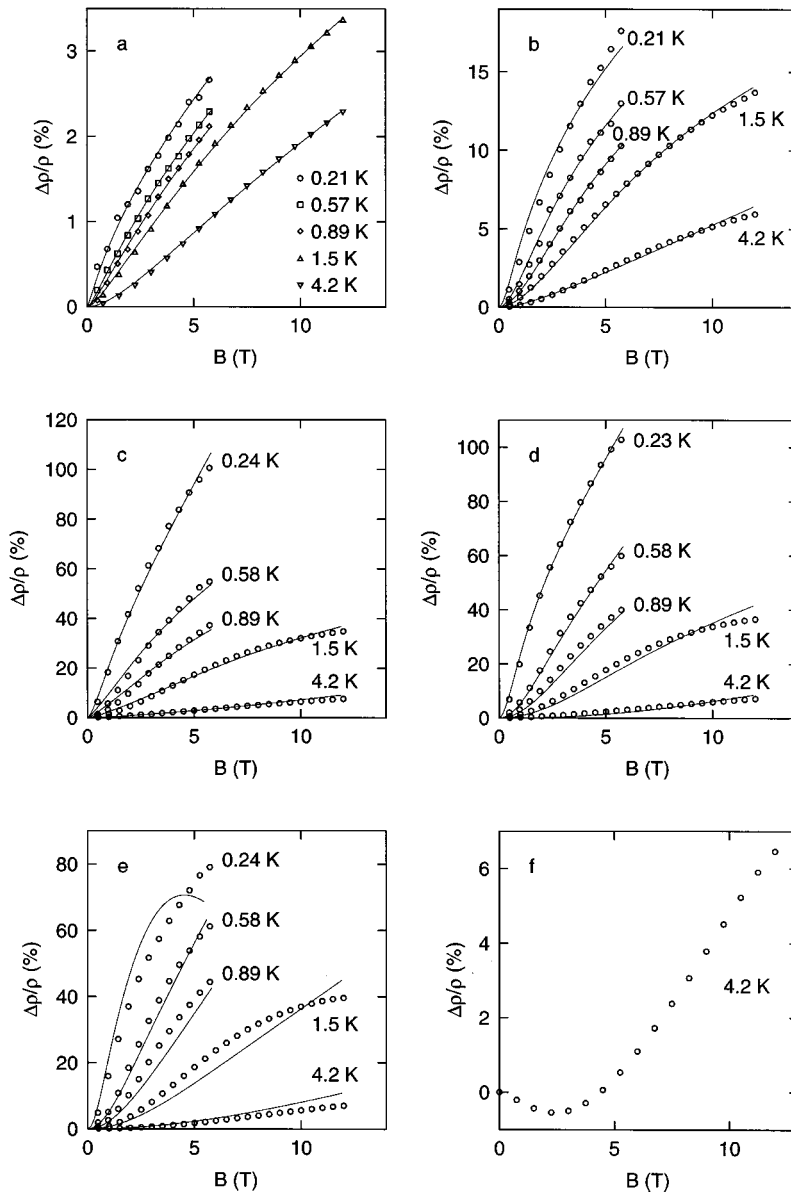


FIG. 2. The magnetoresistance vs magnetic field for six samples of *i*-Al-Pd-Re at the temperatures given in the different panels. The residual resistance ratios R are 2, 4, 11, 13, 23, and 45 in the order of panels (a)–(f). The curves in panels (a)–(e) are calculations from weak localization and electron-electron interaction described in the text.

tude argument illustrates prior to any detailed analysis that the observed MR is qualitatively consistent with QIE in this region of temperatures and resistivities.

However, above a value R_m of the resistance ratio R , which depends on temperature and magnetic field, and in Fig. 3 is in the range 10–23, it can be seen that $\Delta\rho(B,T)/\rho(0,T)$ decreases with increasing ρ and R . Such a maximum is similar to previous observations,^{6,7} and is inconsistent with predictions from weak localization and electron-electron interactions. This behavior is also different from the much slower decrease or constant value of $|\Delta\rho(B,T)/\rho(0,T)|$ with increasing R , observed in insulating oxide systems.^{31,32}

In the region of the change of character of the magnetoresistance, $\rho(4\text{ K})$ for the $R=23$ sample is about 90 m Ω cm compared to about 200 m Ω cm for the $R=45$ sample (Table II). A related change of character at similar resistivities was found recently from a quite different approach.¹ Again without resorting to an analyses of the magnetoresistance in terms of QIE, it was found that the maximum measured $|\Delta\rho(B,T)/\rho(0,T)|$ for a number of different alloys at similar

B and T , including icosahedral quasicrystals, increased in a similar way with increasing $\rho(4\text{ K})$. Above about 100 m Ω cm, this trend was broken, and the maximum magnetoresistance instead decreased with continued increase of ρ .

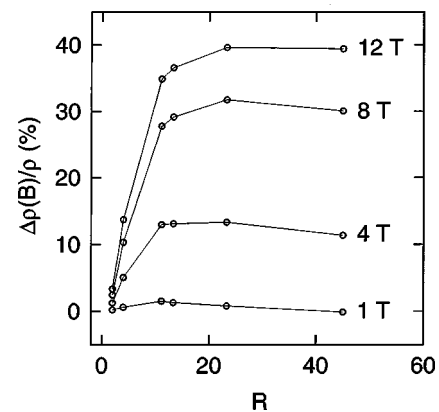


FIG. 3. The magnetoresistance at 1.5 K vs R at the magnetic fields indicated.

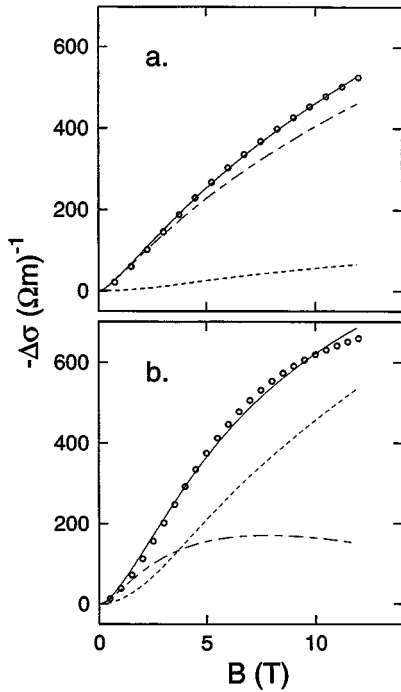


FIG. 4. $-\Delta\sigma$ vs B at 1.5 K for two samples; panel (a) $R=2$, (b) $R=11$. Long-dashed curves show the WL contribution, the short-dashed curves the EEI contribution. The full curve in each panel is the sum of WL and EEI contributions. The figure also illustrates that $|\Delta\sigma|$ increases with increasing ρ in this region of resistivities.

C. Results of analyses

The curves in Fig. 2 show results of analyses (Ia). Good fits to WL and EEI theories were obtained for $R=2-13$, while clear signs of deterioration of this description are apparent for $R=23$. However, the fit in Fig. 2(e) stands out as poor only when compared to the description for lower R values and the superior fits to QIE found in other quasicrystalline systems.¹ In fact, in comparison with results for amorphous metals, the analysis in Fig. 2(e) would still be an acceptable result, particularly when considering that no

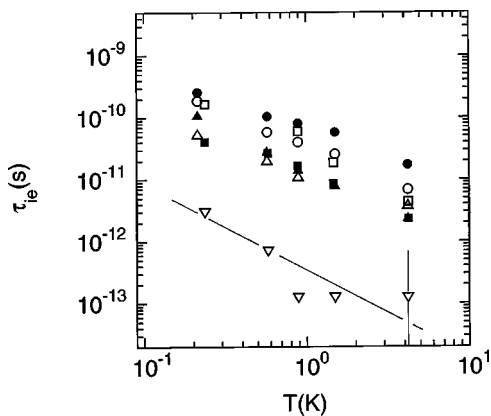


FIG. 5. The inelastic-scattering time τ_{ie} vs temperature for four samples and six analyses. The R values are: circles, 2; up triangles, 4; squares, 11; down triangles, 23. Open symbols, method (Ia); closed symbols, method (II). The error bar for $R=23$ at $T=4.2$ K was estimated as described in text. The straight line for the $R=23$ sample is a guide to the eye, summarizing these data with a slope of $\tau_{ie}(T)$ consistent with those of the other samples.

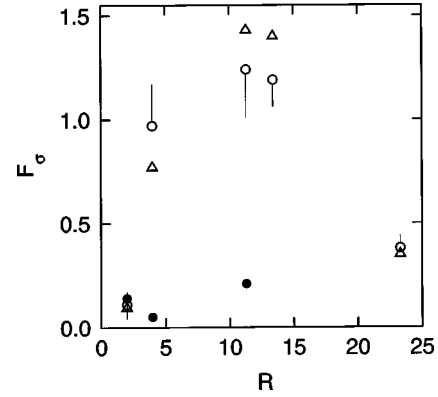


FIG. 6. First analyses of the Coulomb interaction parameter F_σ vs R . \circ , method (Ia); \triangle , method (Ib); \bullet , method (II). The end points of the bars on open circles indicate results for F_σ from analyses (Ia) with $\gamma=0.14$ mJ/mole K² for $R=2$ and 23 and $\gamma=0.20$ mJ/mole K² for $R=4, 11$, and 13.

arbitrary scaling factor adjusting the magnitude of Eqs. (1) and (2) has been introduced.³⁴

Analyses (Ib) gave fits of comparable quality to those shown in Fig. 2. This is the case also for method (II), although in this case only for $R=2, 4$, and 11, while QIE failed for $R \geq 13$. As mentioned, we consider the results from analyses (I) to be more representative.

The limit of about $\rho(4\text{ K}) \approx 100$ mΩ cm thus also corresponds to the beginning of breakdown of the successful descriptions of the MR in terms of QIE obtained for smaller ρ values. For larger $\rho(4\text{ K})$ traditional QIE fail completely. In addition to the present results this trend is also apparent from studies of Mn-doped *i*-Al-Pd-Re,¹¹ where a successful fit to QIE could be made for $x=3$ in Al_{70.5}Pd₂₁Re_{8.5-x}Mn_x but failed for $x=2$. Crude estimates from extrapolations in a graph from Ref. 11 yield $\rho(4\text{ K}, x=3) \approx 60$ mΩ cm and $\rho(4\text{ K}, x=2) \approx 200$ mΩ cm, respectively, in qualitative agreement with the above results. For *i*-Al-Pd-Re of nominal composition Al₇₀Pd_{22.5}Re_{7.5}, a similar trend was qualitatively observed for much larger ρ values with¹² and without¹⁰ substitution of Re by Ru. However, in this case $\rho(4\text{ K})$ at a given R value was larger than for the present samples and those of Ref. 11, which could possibly be due to an extreme sensitivity to Re concentration, or perhaps more likely to cracks in the samples, or other imperfections, leading to an overestimation of the measured ρ .

The WL and EEI contributions in the calculations of $\Delta\sigma$ are exemplified in Fig. 4 for $R=2$ and 11 at 1.5 K. It can be seen that WL dominates at low resistivities and decreases in importance for larger R . The maximum in WL at about $B=7$ T for $R=11$ in Fig. 4(b) reflects a decreasing spin-orbit scattering rate with increasing R , to be discussed below, and already at $R=13$ (not shown) the WL contribution is negative.

Results from these analyses for $\tau_{ie}(T)$ are shown for several samples in Fig. 5. For $R=23$, τ_{ie} falls to 10^{-13} s or below at temperatures above 0.8 K when all measurement temperatures were analyzed simultaneously. Since the analyses are insensitive to changes of τ_{ie} below 0.1 ps, the errors may be considerable, and no lower bound for τ_{ie} of this sample at 4 K is given in Fig. 5. An upper bound for $\tau_{ie}(4\text{ K})$ was estimated by the following procedure: one analyses was

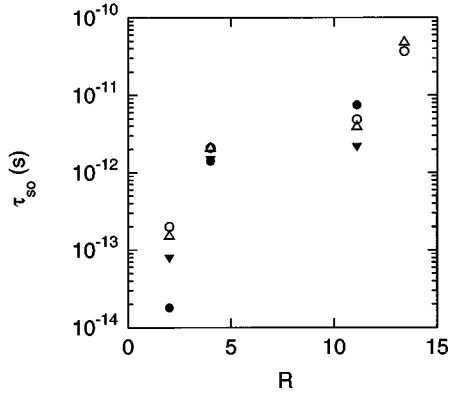


FIG. 7. τ_{so} vs R in different analyses. \circ , method (Ia); Δ , method (Ib); and \bullet , method (II) with $\gamma=0.17$ mJ/mole K^2 . \blacktriangledown , method (II) with $\gamma=0.20$ mJ/mole K^2 . Results from method (Ia) with $\gamma=0.14$ and 0.20 mJ/mole K^2 were similar as described in text.

made with data at 4 K only, a second one with data at 1.5 and 4 K, and so on, until all data in Fig. 2(e) had been included. $\tau_{ie}(4\text{ K})$ varied in the range 0.9 to about 0.1 ps in this process. In this analysis $\tau_{ie}(4\text{ K})$ for the $R=23$ sample would thus be at most 0.9 ps. We also used $\gamma=0.14$ and 0.20 mJ/mole K^2 , corresponding to a change of D of $\pm 20\%$ for several samples. This had a small effect on the results with $\tau_{ie}(T)$ usually remaining within the size of the symbols in Fig. 5.

$\tau_{ie}(T)$ decreases with increasing temperature for all analyses in Fig. 5. The values for an average exponent p in $\tau_{ie}(T)=\tau_0 T^{-p}$ are in the range 1.1–1.5 for different samples and analyses. This is in agreement with standard results for QIE in quasicrystals and corresponds to usual values for electron-electron scattering.¹

The Coulomb interaction parameter F_σ is shown in Fig. 6 as a function of R . There are large differences in results for F_σ between methods (I) and (II), and any conclusion as to the magnitude is uncertain. With the larger ρ of method (II), D is smaller, leading to a larger contribution from WL, and therefore reduced EEI contribution and smaller F_σ . Since as mentioned, QIE are likely present in ρ above 4 K, the small F_σ 's in method (II) may be an artifact. Furthermore, since the analyses are made in a region of large magnetoresistance the possibility of numerical instabilities should also be noticed.

Some different analyses to check on the reliability of the results for F_σ are shown in Fig. 6 and described in the caption. However, the question whether there is a maximum at intermediate R values relies strongly on the results for the $R=23$ sample, where the fits of QIE are the least good [Fig. 2(e)]. The discussion of this point is deferred until a closer examination of the analyses of the $R=23$ sample has been in Sec. IV.

The spin-orbit scattering time τ_{so} is usually the most difficult parameter to determine from analyses of QIE, and results differing by a factor of 10 or more are common. The results are presented in Fig. 7. Several different analyses were again performed. The large sensitivity of the results for τ_{so} in method (II) to variations in γ is illustrated in the figure and can probably be traced again to the sensitivity to D for small D . Similar variations of γ in method (I) gave small

variations. For instance, for $\gamma=0.17\pm 0.03$ mJ/mole K^2 , τ_{so} was 0.2 ± 0.04 ps at $R=2$ and at $R=13$ the results were $\tau_{so}=37$ and 44 ps for $\gamma=0.17$ and 0.20 mJ/mole K^2 , respectively. Figure 7 gives evidence from both methods (I) and (II) that τ_{so} increases with increasing R and $\rho(4\text{ K})$ in i -Al-Pd-Re up to at least $R=11$, or $\rho(4\text{ K})\approx 30$ m Ω cm. However, the figure also illustrates that the rate of this increase is quite uncertain.

When results for the $R=23$ sample are included, indications are that τ_{so} continues to increase. However, the analyses are quite insensitive to variations of τ_{so} in this case, and an error up to a factor of 100 is conceivable. These data have therefore been omitted in Fig. 7. Two circumstances may contribute to this large error. First, when the quality of fits to QIE starts to deteriorate, as for the $R=23$ sample, one can expect that information on τ_{so} is the first to be lost, in concordance with the well-known difficulties with this parameter. Furthermore, the results for R in the range 2–13 indicate an increasing τ_{so} with increasing R . A continuation of this trend up to $R=23$ implies a vanishing spin-orbit interaction, resulting in extreme insensitivity to large τ_{so} in numerical analyses.

In summary of these analyses of τ_{so} we thus find indications for a decreased spin-orbit scattering rate with increasing R in samples up to $R=13$. However, the errors increase with increasing R and for $R=23$ we can only conclude that a continued decrease of τ_{so}^{-1} is consistent with data but cannot be proven.

IV. EMERGING BREAKDOWN

A. Analyses in variable temperature regions

Based on the empirical fact that analyses of the magnetoresistance, in terms of QIE, in their range of validity usually give excellent descriptions of the observations in quasicrystals, one can expect to obtain further information on the nature of the beginning deterioration in Fig. 2(e) from more detailed analyses. Our starting point is the assumption that at $R=23$ it may be unfounded to include all temperatures between 0.2 and 4.2 K in the analyses. The apparent breakdown of QIE may be associated with the approach to a metal-insulator transition. One could then expect that novel contributions to MR from the insulating side of the transition start to contribute and that such contributions would be observable below a temperature that increases when moving further into the insulating side. If nonmetal contributions to MR are present in a particular sample close to the MIT, they would therefore primarily manifest themselves at the lowest-measurement temperatures.

To investigate this idea, the MR of all the samples was reanalyzed for different temperature ranges. The notation

$$A_{4.2\text{ K}}^{T_m}$$

will be used for an analysis of type (Ia) where all measurement temperatures between 4.2 K and T_m were included. Two new choices of T_m were made, 1.5 and 0.9 K. The analyses in Fig. 2 correspond to $T_m=0.2$ K. When only metallic contributions are present, and with a reasonable extrapolation of $\tau_{ie}(T)$, the analysis $A_{4.2\text{ K}}^{T_m}$ will describe data also below T_m . If other contributions are present below T_m , systematic deviations between $A_{4.2\text{ K}}^{T_m}$ and observations would be expected below T_m for similar calculations.

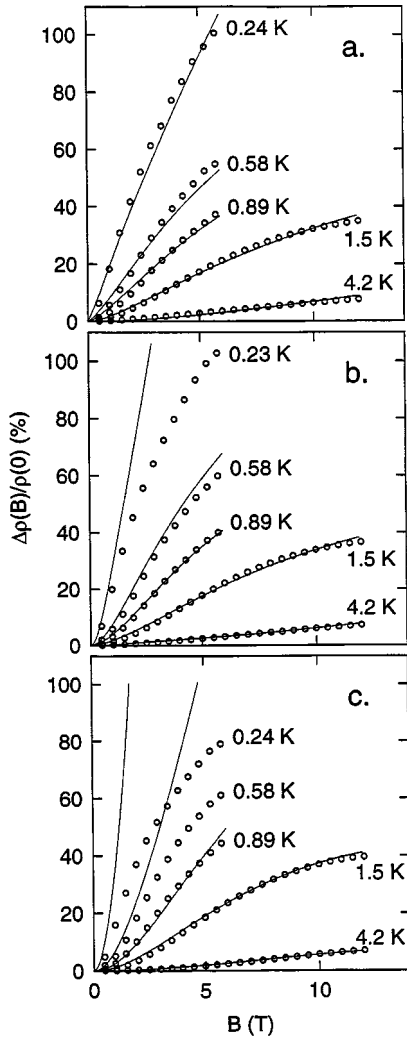


FIG. 8. Magnetoresistance vs B : panel (a) $R=11$, (b) $R=13$, and (c) $R=23$. The full curves in each panel are analyses in terms of QIE using results at 0.89, 1.5, and 4.2 K only with good fits at these temperatures for all samples. The curves at 0.6 and 0.2 K are extrapolated calculations described in text. Deviations between data and calculations emerge at 0.2 K for $R=13$, and increase in magnitude for $R=23$. These results indicate an additional negative contribution to the magnetoresistance.

The results with $A_{4.2\text{K}}^{0.9\text{K}}$ for samples $R=11$, 13, and 23 are shown in Fig. 8. Excellent descriptions of data were obtained at the three temperatures of the analyses. Similar good descriptions were also obtained for $A_{4.2\text{K}}^{1.5\text{K}}$. In Fig. 8(a) the quality of the fit for $R=11$ is comparable to those in Fig. 2(c) at 0.9, 1.5, and 4.2 K. For $R=13$ the fits for the same temperatures are somewhat improved in Fig. 8(b) compared to Fig. 2(d), while for $R=23$, they are markedly improved at all three temperatures in Fig. 8(c) and of quality comparable to the other samples in Fig. 8 and in Fig. 2.

The curves at 0.24 and 0.58 K in Fig. 8 were obtained by extrapolating $\tau_{ie}(T)$ linearly according (or corresponding) to Fig. 5, and calculating QIE with the results for the other parameters obtained at $T \geq 0.89$ K. These results are not sensitive to variations in the extrapolation, and allowing instead $\tau_{ie}(T)$ to saturate at lower temperatures gave negligible differences. At $R=11$ the data at 0.58 and 0.24 K are well

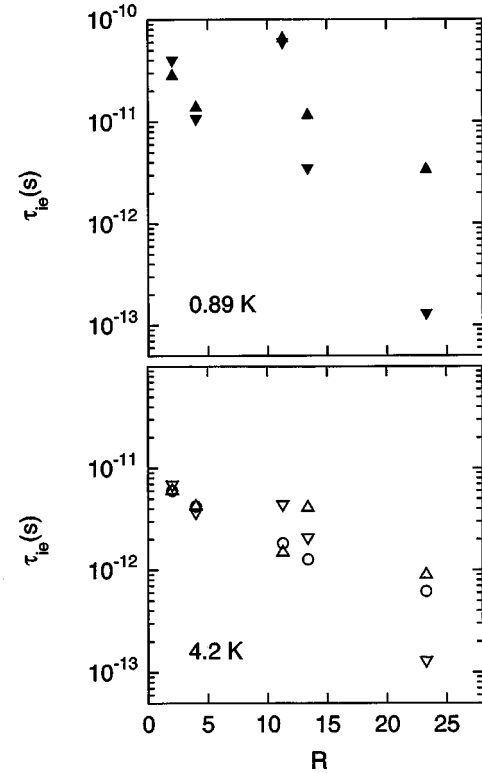


FIG. 9. τ_{ie} vs R at 0.89 and 4.2 K. Down triangles: $A_{4.2\text{K}}^{0.2\text{K}}$, up triangles: $A_{4.2\text{K}}^{1.5\text{K}}$, circles: $A_{4.2\text{K}}^{4.2\text{K}}$. A decrease of τ_{ie} with increasing R is apparent at both temperatures. At 4.2 K an average value of this decrease is a factor of $30 \pm 50\%$ in the range from $R=2$ to 23.

described by the analyses at $T \geq 0.89$ K. For $R=13$ there are deviations at 0.23 K, and at $R=23$ these deviations are of larger magnitude and are observable already at 0.58 K.

QIE can thus well describe the MR between 0.9 and 4.2 K for all samples in the range from $R=2$ to 23. For $R \geq 13$ deviations appear at 0.2 K suggesting a negative contribution to MR. Qualitative support is thus found that a contribution from a negative MR on the insulating side of an MIT emerges at 0.2 K for $R=13$ and increases in magnitude up to (at least) $R=23$.

B. Decrease of τ_{ie} with increasing R

Inspection of Fig. 5 shows that there is a tendency for the inelastic-scattering time $\tau_{ie}(T)$ to decrease with increasing R and $\rho(4\text{K})$ in both analyses (I) and (II). Results for τ_{ie} vs R are shown in Fig. 9 at $T=0.9$ and 4.2 K for the three analyses $A_{4.2\text{K}}^{T_m}$ with $T_m=0.2, 0.9$, and 1.5 K. An overall decrease of τ_{ie} with increasing R is found in all analyses at 4.2 K, and a similar trend is also apparent at 0.89 K. The scatter of the results for τ_{ie} is observed to increase both as a function of increasing R at both temperatures and at 0.9 K, as compared to 4.2 K, in qualitative agreement with the discussion above on the emergence of breakdown of QIE.

The rate of decrease of τ_{ie} with increasing R is accordingly difficult to determine. When R increases from 2 to 23, one can estimate within an uncertainty of 50% that τ_{ie} at 4.2 K decreases by about a factor of 30 for the three analyses in Fig. 9. A similar rate is consistent with the results at 0.9 K, although here the scatter is large. Excluding the lower value

of τ_{ie} at $R=23$, the most uncertain datum in the panel, a decrease of τ_{ie} by a factor of 10 seems more likely.

Matsuo *et al.*³⁵ derived an expression for the weak-localization magnetoresistance, applicable to the case when the condition $\tau_{ie} \gg \tau$ is weakened to $\tau_{ie} > \tau$, which in addition to the parameters of Eq. (1) also contains τ . One might ask if this approach would better describe $\Delta\rho(B,T)/\rho(0,T)$ for $R=23$ at $T < 0.89$ K. In addition, direct estimates of τ could then be obtained. However, this possibility does not seem to be relevant here. For a given sample, with constant τ , the condition $\tau_{ie} \gg \tau$ would not breakdown for decreasing temperature but improve, in contrast to the deviations observed in Fig. 8 for decreasing temperatures. Anyway, our efforts to handle the expression of Matsuo *et al.* with 18 terms in $\Delta\rho(B,T)/\rho(0,T)$ have failed, and results were obtained that did not appear to be physically reasonable.²

The ρ dependence of τ_{ie} does not seem to have been discussed previously in the literature on QIE in quasicrystals. From some published results a similar trend in $\tau_{ie}(\rho)$ can be found, however. In Ref. 2, the magnetoresistance of two *i*-Al-Cu-Fe samples with $\rho(4$ K) of 4.5 and 10 m Ω cm were analyzed over a wide temperature range. The large- ρ sample was found to have a significantly smaller τ_{ie} than the small- ρ sample over a temperature range from below 1 K to about 80 K. In Ref. 11, the magnetoresistance of Al_{70.5}Pd₂₁Re_{8.5-x}Mn_x with $x=3, 4$, and 5 was described in terms of QIE in a temperature range from 1.5 to 10 K. For this series of x , $\rho(4$ K) was roughly 60, 35, and 30 m Ω cm, respectively. Again a significantly smaller τ_{ie} was found for the high-resistivity sample with similar results for the two low- ρ samples. These results confirm the present findings, and suggest that a decreasing τ_{ie} with increasing ρ may be a general property in these resistive icosahedral alloys. It should be noted, however, that this relation between τ_{ie} and ρ is expected to be alloy-system dependent due to the differences between different quasicrystalline alloy systems in, e.g., atomic scattering potentials and in the density of states and other band-structure properties.

C. Spin-orbit scattering and Coulomb interaction

The results for τ_{so} from the analyses in Sec. IV A are more uncertain than those described in Fig. 7. For analysis $A_{4.2\text{ K}}^{1.5\text{ K}}$ this is not surprising since the usual insensitiveness to variations in τ_{so} is compounded by the numerical flexibility occurring when only two temperatures are used to describe $\Delta\rho(B)/\rho$ vs B with the free parameters of Eqs. (1) and (2). For $A_{4.2\text{ K}}^{0.9\text{ K}}$, an increase of τ_{so} with increasing R is confirmed, but the rate is smaller than in Fig. 7. For the $R=23$ sample little can be said about τ_{so} , as discussed above. Most analyses give results within the huge range of $\log_{10} \tau_{so} = -10 \pm 1.7$, where numbers in excess of -9 cannot be distinguished and indicate vanishing spin-orbit interaction.

A lower bound for the increase of τ_{so} in the range from $R=2$ to 11 is of order a factor of 5 in τ_{so} . This appears to be much too strong to be explained by an effect of the mass Z , even for an exponent α in $\tau_{so}^{-1} \sim Z^\alpha$ as large as 12, as sometimes used.³⁶ It would require concentration changes in excess of 1 at. %, which seems to be unreasonably large.

From the calculations by Millis and Lee,³⁷ it is expected that F_σ is suppressed for strong spin-orbit scattering. This

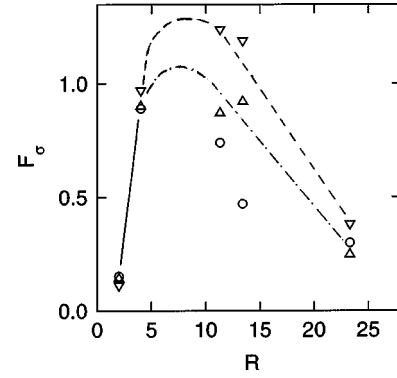


FIG. 10. Second analyses of the Coulomb interaction parameter F_σ vs R . ∇ , analysis $A_{4.2\text{ K}}^{0.2\text{ K}}$; \triangle , $A_{4.2\text{ K}}^{0.9\text{ K}}$; \circ , $A_{4.2\text{ K}}^{1.5\text{ K}}$. A strong decrease of F_σ for increasing $R > 10$ is apparent in all analyses. The curves are guides to the eye summarizing data for two of the analyses.

prediction has been verified in amorphous metals by doping with a heavy element.³⁸ The present results for τ_{so} and F_σ indicate such a correlation, with an increase in both parameters for a range of R values from 2 to about 13 in Figs. 6 and 7. From published results on quasicrystals one can again find some support for the trend observed in the present data. Thus in a study of the MR of two samples of *i*-Al-Cu-Fe, the larger resistivity was associated with a larger F_σ as well as a larger τ_{so} .² On the other hand, in two *i*-Al-Pd-(Re-Ru) samples with R of 3 and 10,¹² the results for the MR showed a constant F_σ within $\pm 15\%$, while a larger τ_{so} was found for the less-resistive sample. A smaller Lande factor g^* was obtained for the more-resistive sample. With two additional adjustable parameters however, g^* and the magnitude of the calculated MR, the increased flexibility would make it difficult to ascertain trends in the results for the parameters.

We now discuss if the apparent maximum in F_σ vs R in Fig. 6 can be supported. As mentioned, this result was primarily based on the $R=23$ sample in some different analyses of the type $A_{4.2\text{ K}}^{0.2\text{ K}}$, which are less good than the others. Results for F_σ are comparatively stable in analyses of QIE. The method in Sec. IV A then provides a handle to this problem, since analyses $A_{4.2\text{ K}}^{1.5\text{ K}}$ and $A_{4.2\text{ K}}^{0.9\text{ K}}$ are of similar quality as the other fits.

The results of the analyses $A_{4.2\text{ K}}^{T_m}$ with $T_m=0.2, 0.9$, and 1.5 K are shown in Fig. 10. In all cases F_σ increases for increasing small- R values, passes through a maximum, and decreases for larger- R values. The height and R value of the maximum decrease when T_m in the analyses increases, but at $R=23$ a low value of F_σ in the range 0.25–0.38 is found in all cases. The scatter of the results is the largest for $A_{4.2\text{ K}}^{1.5\text{ K}}$ since only two temperatures enter in those analyses. The results in Fig. 10 give evidence that F_σ decreases with increasing resistivity in the region where QIE start to break down.

When approaching a metal-insulator transition, the Thomas-Fermi screening length is expected to diverge^{39,40} and F_σ would $\rightarrow 0$. Our observation of a decreased F_σ may reflect that an MIT is approached for $\rho(4$ K) in excess of about 90 m Ω cm in *i*-Al-Pd-Re.

For τ_{so} , as mentioned, it is difficult to draw any conclusions about the development for the larger R . Not only are the analyses in terms of QIE in this region insensitive to variations in τ_{so} , in addition the influence of τ_{so} on the mag-

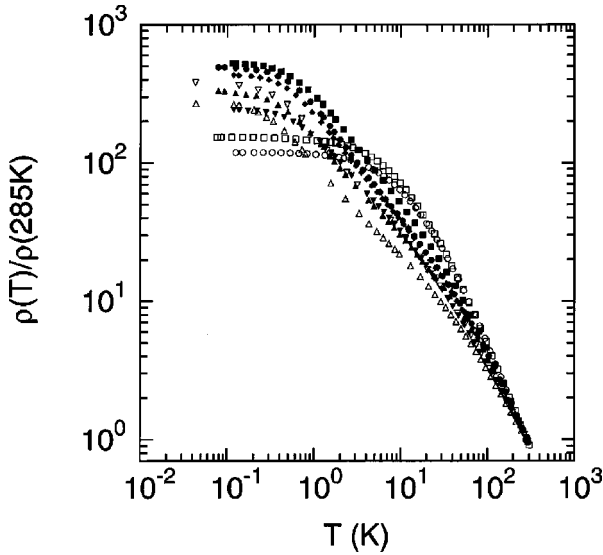


FIG. 11. The resistivity normalized at 285 K, $\rho(T)/\rho(285\text{K})$ vs temperature for *A* and *B* samples with the following *R* values: *A* samples: \blacksquare 107, \bullet 83, \blacklozenge 77, \blacktriangle 56, \blacktriangledown 62, and *B* samples: ∇ 60, \triangle 40, \square 119, \circ 98.

netoresistance when approaching an MIT or passing into a variable-range-hopping (VRH) region is extremely controversial.^{41–45} In particular opposite effects of τ_{so} on the sign of $\Delta\rho(B,T)/\rho(0,T)$ has been predicted. From a random-matrix approach Pichard *et al.* found a positive MR for spin-orbit scattering systems, while MR should be negative in the absence of spin-orbit scattering.⁴¹ Meir *et al.*, on the other hand, used an analytic independent-path formalism and found a negative MR for all spin-orbit scattering strengths.⁴² Medina and co-workers examined the interference between forward-scattering paths and found a negative MR with a weak increase of the localization length ξ in magnetic field without spin-orbit scattering,⁴³ and with spin-orbit scattering a negative MR with constant ξ .⁴⁴ From numerical studies of the Hubbard model with disordered on-site energies, Eto, on the other hand, found that the MR is negative in the absence of spin-orbit interaction while spin-orbit interaction can give rise to a positive MR at low magnetic fields changing sign to negative MR at high fields.⁴⁵

In view of these experimental as well as theoretical difficulties we can only give a few possible scenarios for interpreting the results for $R \leq 23$. Figure 7 suggests the possibility that spin-orbit scattering vanishes for increasing resistivity in *i*-Al-Pd-Re. In fact, a negative weak-localization contribution to MR develops in our analyses already at $R = 13$ for $T \geq 0.89$ K. One could then view the results as a precursor to a negative MR in the VRH region, similar to the approach by Shapir and Ovadyahu from experiments on Au-doped indium-oxide films on both sides of the MI transition.⁴⁶ These authors concluded that within the backscattering picture, disorder reduces both the phase coherent and the spin-orbit scattering in the MR. A problem with this interpretation for *i*-Al-Pd-Re is of course, that for larger *R* and ρ the MR at low temperatures is negative only in the low-*B* region [Fig. 2(f) and Sec. V], which thus would seem to call for further contributions to MR for large *B* and ρ at low temperatures.

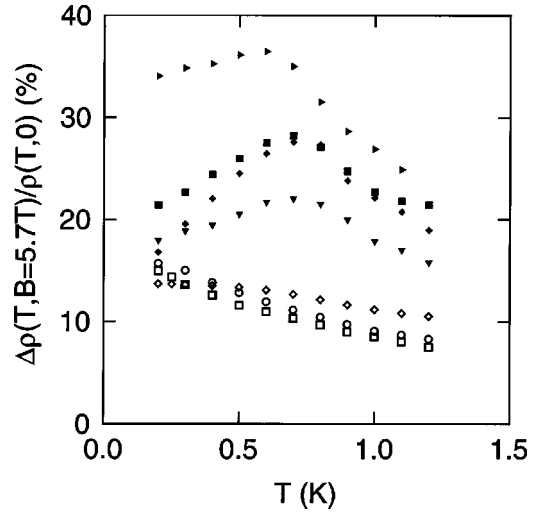


FIG. 12. The magnetoresistance at low temperatures and $B = 5.7$ T for samples with the following *R* values; *A* samples: \blacktriangleright 48, \blacksquare 107, \blacklozenge 77, \blacktriangledown 62, and *B* samples: \diamond 75, \circ 98, \square 119.

A sign change from negative to positive MR with increasing *B* has been observed in *n*-type GaAs in the VRH regime,⁴⁷ and was accounted for in a model by Fukuyama and Yosida⁴⁸ considering Zeeman splitting among Anderson localized states. When this model is applied to *i*-Al-Pd-Re, a major difficulty is that no variable-range-hopping regime was observed down to 30 mK for samples with $R < 60$.¹⁹ On the other hand, a VRH region has recently been found in similarly prepared *i*-Al-Pd-Re samples below 0.6 K for *R* values in the range 84–128.¹⁶

Finally, in analyses such as ours, where weak localization provides the only source of a negative MR, a severe overestimation of τ_{so} could result when a negative contribution from the insulating side appears. We must thus ask if models for the MR with strong spin-orbit scattering could be relevant. The analyses in Sec. IV B indicate that this is not the case. By analyses in reduced sets of temperatures a smaller value of τ_{so} for $R = 23$ is found in concordance with this argument. However from both analyses $A_{4.2\text{K}}^{1.5\text{K}}$ and $A_{4.2\text{K}}^{0.9\text{K}}$, τ_{so} ($R = 23$) is about 2 ps, at the lower end of the interval for τ_{so} given above, which is still a comparatively weak spin-orbit scattering.

V. HIGH-RESISTIVITY REGION

A. Temperature dependence of the resistivity

In this section, results for the magnetoresistance will be described for samples prepared by two different methods and with *R* values ≥ 50 , roughly corresponding to $\rho(4\text{K}) > 300$ m Ω cm. The overall temperature dependence of ρ of these samples provides a convenient sample characterization, and is first briefly discussed.

The temperature dependence of the normalized resistivity, $\rho(T)/\rho(285\text{K})$, is shown in Fig. 11. The figure illustrates the significant point that the temperature dependence of $\rho(T)$ of *A* and *B* samples is similar at temperatures above a few K over a variation of about two orders of magnitude in ρ for samples of equivalent *R* values. This overall similarity between the different samples conveys a particular interest to

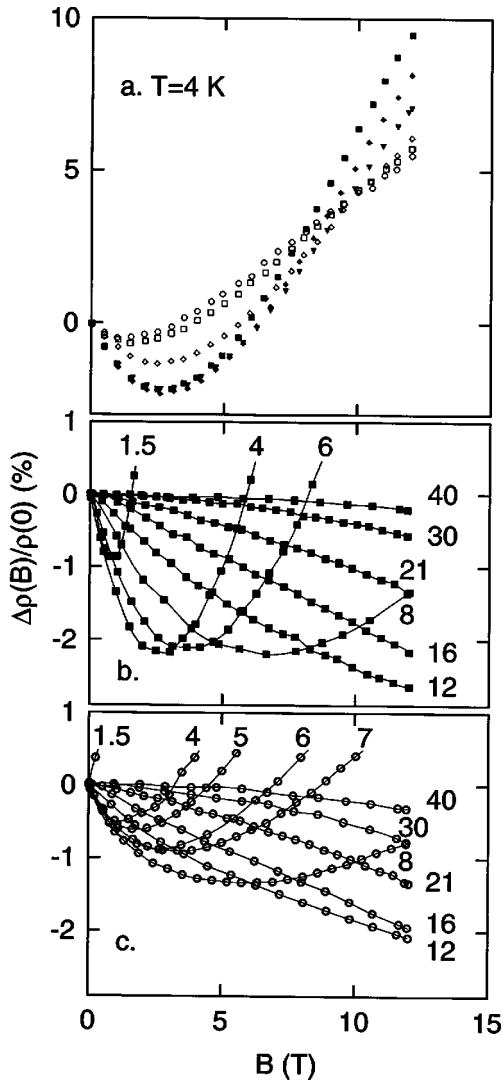


FIG. 13. (a): The magnetoresistance at 4 K for samples with different R values. A samples: \blacksquare 107, \blacklozenge 77, \blacktriangledown 62, and B samples: \diamond 75, \square 119, \circ 98. (b) and (c): The magnetoresistance at the temperatures indicated (in K) from 1.5–40 K.

the differences in the magnetoresistance observed at lower temperature, to be described below.

Some differences in $\rho(T)$ are also illustrated in Fig. 11. Below 4 K the A samples have a stronger temperature dependence than the B samples, but all samples seem to saturate at low temperatures in this range of temperatures. The overall temperature dependence $\rho(100 \text{ mK})/\rho(285 \text{ K})$ is therefore stronger in the A samples than in the B samples. The A samples show an increase of $\rho(100 \text{ mK})/\rho(285 \text{ K})$ with increasing R values. This is not observed in the B samples, where, e.g., samples with $R > 75$ have a lower $\rho(100 \text{ mK})/\rho(285 \text{ K})$ than samples with smaller R values. There is a trend for all samples that the temperature at which the resistivity saturates is higher for samples with a larger resistance ratio. This effect is most evident in the B samples. For the most resistive B samples, as mentioned measurements down to 20 mK suggest that the saturation is only a plateau followed by a sharp increase in resistivity at low temperatures indicating a Mott VRH conductivity.¹⁶ However, the reason for this temperature dependence at low temperatures is not fully understood.

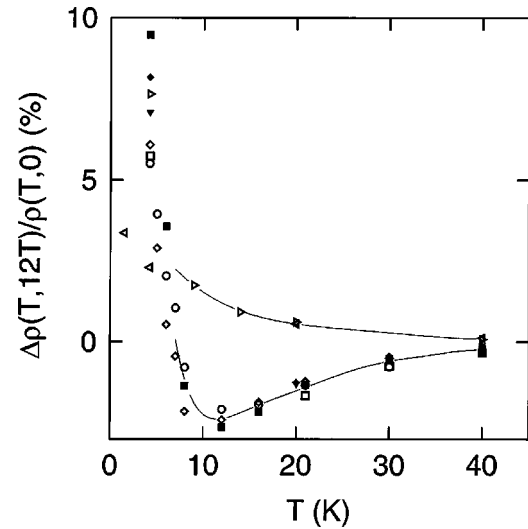


FIG. 14. The magnetoresistance at 12 T vs T for samples with different R values. A samples: \blacksquare 107, \blacklozenge 77, \blacktriangledown 62, and B samples: \triangleleft 2, \triangleright 11, \diamond 75, \square 119, \circ 98. The curves are guides to the eye for samples with $R \geq 62$, bottom curve, and $R \leq 11$, top curve, respectively.

B. Magnetoresistance

The magnetoresistance of samples with $R > 50$ is shown at low temperatures, $T < 1.5 \text{ K}$, and at $B = 5.7 \text{ T}$ in Fig. 12. The MR is larger in the A samples and possesses a maximum in $\Delta\rho(T, B)/\rho(T, 0)$ at about 0.6–0.7 K. $\Delta\rho(T, B)/\rho(T, 0)$ in the B samples increases with decreasing temperature, but remains smaller at all fields and temperatures measured compared to the A samples.

The magnetoresistance at higher temperatures is illustrated in Fig. 13. In panel (a), $\Delta\rho(B)/\rho(0)$ at 4 K is displayed for different samples. At high-magnetic fields $\Delta\rho(B)/\rho(0)$ is large and positive. As temperature further increases the magnetoresistance at 12 T decreases down to a minimum value of approximately 2.5% at 12 K and thereafter approaches zero as the temperature is further increased,

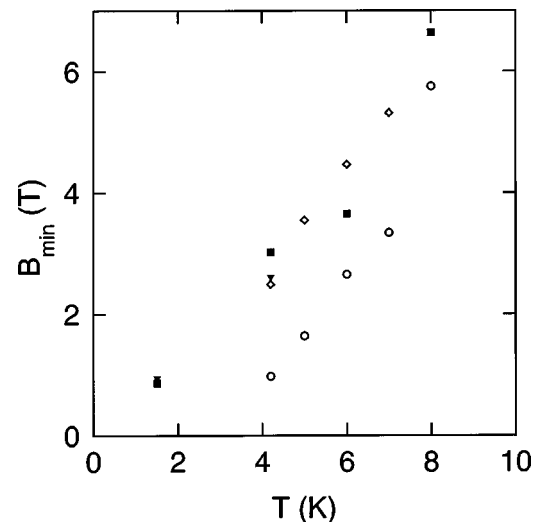


FIG. 15. B_{\min} vs T for samples with different R values. A samples: \blacksquare 107, \blacktriangledown 62, and B samples: \triangleleft 75, \circ 98. B_{\min} is the field at which $\Delta\rho(B)/\rho(0)$ has a minimum.

Figs. 13(b), 13(c), and 14. This is in contrast to the samples with low- R values, as can be seen in Fig. 14 for $R < 11$ at 12 T. For these samples $\Delta\rho(B)/\rho(0)$ is positive for all fields and temperatures ≤ 40 K.

C. Sample differences

Although the A and B samples have the same nominal composition and similar R values there are significant differences in the temperature and magnetic-field dependence. As described above, $\rho(T)$ increases more strongly in the A samples at low temperatures and the MR is larger and with a different temperature behavior at low temperatures. The differences in the SEM pictures are substantial (Fig. 1). There are voids and more secondary phase in the A samples than in the B samples. We must ask the question, how does this correlate to the transport properties? Any metallic secondary phase would be expected to weaken the temperature dependence of $\rho(T)$, while $\rho(T)$ instead depends more strongly on temperature in samples with more secondary phase. Furthermore, a metallic phase would not influence the MR on this scale. As mentioned, the systematic increase in MR with R for moderately large R in Fig. 3 could not be likely caused by these differences. There is a possibility that the secondary phase is insulating. To our knowledge, there have been no reports that Al-Re is an insulator, even if it cannot be excluded since one crystalline Al-Ru phase has been reported to be insulating.⁴⁹ In view of these observations it seems most probable to conclude that the secondary phase does not cause the differences in the observed $\rho(T)$ and $\Delta\rho(T,B)/\rho(T,0)$ for the two sets of samples. The nature of possible defects of concentration differences, presumably of the icosahedral phase, which might cause these differences, must be studied further.

D. Minimum in the magnetoresistance

$\Delta\rho(B)/\rho(0)$ has a minimum at temperatures between 1.5–8 K and 4–8 K for the A and B samples, respectively, for $R \geq 60$, Figs. 13(a)–13(c) and 15. The value of $|\Delta\rho(B)/\rho(0)|_{\min}$ is approximately the same for all A samples at $T \geq 4$ K, but is more sample dependent and smaller in the B samples, as can be seen in Fig. 13. The magnetic field at which this minimum occurs, B_{\min} , increases roughly linearly as the temperature increases. At temperatures above 8 K, $\Delta\rho(B)/\rho(0)$ shows a monotonous decrease up to the maximum field applied, 12 T. The temperature dependence of B_{\min} vs T is shown in Fig. 15. It seems likely that it is the same mechanism causing the negative part of the MR at temperatures below 8 K as the negative MR at higher temperatures. The approximately linear relation between T and B_{\min} for each sample can be described by the function $(B_{\min} + B')/T = a$, with B' varying between samples from 0 to 3 T. The factor a is roughly the same for all samples, and ≈ 0.9 T/K.

The Zeeman effect is appreciable when $g^* \mu_B B > k_B T$,⁵⁰ where g^* is the Landé factor, μ_B the Bohr magneton, and k_B the Boltzmann constant. With $g^* = 2$ this corresponds to $B/T > 0.7$ T/K. It therefore seems plausible that the positive slope is related to the Zeeman term in the relevant transport theory and becomes sizable as B/T increases above 0.7 T/K.

However, this is speculative at present and the relevant transport mechanism is still unknown.

E. Possible metal-insulator transition

As mentioned, some results for the resistance at low temperatures in i -Al-Pd-Re samples with large $\rho(4$ K) and R ,^{11,16} may indicate that a metal-insulator transition has been passed in some samples as a function of some microscopic parameter, which presumably can be reflected by ρ , and R . If so, it should be possible to monitor such an MIT in $\Delta\rho(T,B)/\rho(T,0)$ as well.

Theories for conventional QIE break down when the resistivity increases above $\rho(4$ K) ≈ 0.1 Ω cm as discussed above. There are also theories of the MR on the insulating side of the MIT, i.e., in the strongly localized regime. However, in between these regimes there are no theories that could account for the transport properties. One could expect that at finite temperatures the mechanisms in both the weakly and strongly localized regimes apply in a transitional regime, but with reduced magnitudes. The analyses in Sec. IV above may illustrate such a behavior with a new negative contribution appearing as an additional term in traditional QIE analyses.

If one can extrapolate the trend for the spin-orbit scattering rate τ_{so}^{-1} and Coulomb interaction F_σ vs R from Sec. IV to these samples of higher R values one may conjecture that F_σ is small and the spin-orbit scattering weak. As mentioned, a small F_σ may be associated with an approaching MIT, since in the picture of Thomas-Fermi screening the Hartree term will decrease to zero as the screening length diverges at the MIT.³⁹ However, τ_{so}^{-1} in the region of an MIT is not understood. Examples were discussed above on differing views of the role of spin-orbit scattering and the expected sign of the MR.^{41–45} This question remains controversial also irrespective of the strength of τ_{so}^{-1} . E. g., Sivan *et al.*⁵¹ predict a positive MR close to the MIT and a negative MR well on the insulating side of the MIT for all τ_{so}^{-1} , and theories such as variable-range hopping and nearest-neighbor hopping predict a positive magnetoresistance due to shrinking of wave functions as the magnetic field is increased.⁵² The large number of theories suggested for insulators makes it difficult to make any quantitative conclusions about the MR.

The trend with a minimum in the MR's field dependence has been observed earlier in systems close to and on both sides of the MIT.^{47,53,54} In the results of Ref. 54 for oriented poly(phenyl-enevinylene), the negative part of the MR vanishes as the metal-to-insulator transition is passed. The behavior of the MR was attributed to an interplay between weak localization and electron-electron interaction and it was concluded that the samples are in the metallic regime due to the absence of a strong positive MR. In Ref. 53, MR is negative on the insulating side, and remains negative further into the insulator when the doping of the GaAs samples decreases. Benzaquen *et al.*⁴⁷ have analyzed their measurements of the MR in terms of a positive part due to shrinking of wave functions in magnetic field,^{52,55} and a negative part due to Zeeman splitting in the variable-range-hopping regime.⁴⁸ It may not be justifiable to apply these theories to our data, since we do not know when we are on the insulating side of an MIT. It is also impossible to check the reli-

ability of the analyzed values. We have nevertheless made an analysis in terms of these theories in an *A* sample with $R = 107$ and in a *B* sample with $R = 98$ at 6 K. Both analyses resulted in comparable fits and parameters. The minimum in $\Delta\rho(B)/\rho$ can possibly be understood within this theory, as illustrated in Fig. 16 for the *A* sample. However, if the field dependence up to 12 T was fitted, the MR diverged to large positive values at strong fields. Furthermore, an attempt to include several temperatures and the temperature-dependent part in the expression of Ref. 47 was not successful.

In the present Al-Pd-Re samples it seems likely that the transport mechanisms in a possible insulating regime would be affected by interference effects, since weak localization and electron-electron interaction are the dominating effects in the low-resistivity samples. According to Meir *et al.*⁴² the interference effects on the insulating side lead to a negative part in the MR well on the insulating side and a positive part close to the MIT.

One possibility to interpret the results in Figs. 12, 13(b), and 13(c) is that contributions from a possible MIT are increased as the temperature is decreased. In that picture the negative part of the MR is due to weak localization, with weak spin-orbit interaction, and an absence of electron-electron interaction. Approaching an insulating state with decreasing temperature the WL contribution breaks down and an apparent new positive part in the MR becomes dominant for samples in this high-resistivity range, resulting in an increasing positive MR.^{42,51} As temperature further decreases the MR in the *A* samples passes a maximum, Fig. 12, and starts to decrease in qualitative agreement with Ref. 51. If this interpretation is correct, it would suggest that the *A* samples are more insulatinglike than the *B* samples, which is consistent with the stronger temperature dependence of the resistivity at low temperatures. The trend that the MR should exhibit a maximum in the magnetic-field dependence of the MR as suggested in Ref. 51 is, however, not observed.

VI. BRIEF CONCLUSIONS

The magnetoresistance has been studied in icosahedral Al-Pd-Re with residual resistance ratios R from 2 to 120. For samples with $R \leq 23$, MR is positive from 0.2 to 4 K in fields up to 12 T. The form of MR is similar to conventional results for QIE in metals with diffusively scattered electrons, albeit at $R = 11$ and 13, the magnitude is exceptional, exceeding 100% at low temperatures.

As long as the temperature dependence of $\sigma(T)$ in the resistive quasicrystals is not understood, it would seem unfeasible to determine the background conductivity σ_0 to which QIE should be added. This difficulty has to some extent been hedged by using two different methods of analyses. The common trends found in these analyses over a range of R for some parameters of QIE, give increased confidence to our results.

The analyses of $\Delta\rho(B)/\rho$ suggest that τ_{ie} decreases with increasing R and resistivity in a range of R from 2 to 23. From analyses over reduced ranges of temperatures, information was obtained on some details of the breakdown of QIE at large R . The appearance of a new negative contribution to MR, which increases in magnitude with increasing R , and the likely decrease of F_σ for large R suggest that an MIT is

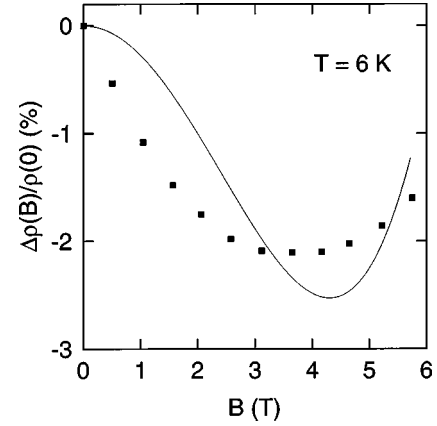


FIG. 16. The magnetoresistance at 6 K up to 6 T for an *A* sample with $R = 107$. The curve is a fit to a theory of Benzaquen *et al.*⁴⁷ with the fitted parameters $K_s = 3.7 \times 10^{-3} 1/T^2$ and $a_1 = 0.13 1/T$ in the notations of Ref. 47.

approached. In the range from $R = 2$ to 11, τ_{so}^{-1} decreases and F_σ increases, in agreement with the expectation from calculations of spin-splitting effects on the magnetoconductivity in materials with spin-orbit scattering.³⁷ At $R = 23$, τ_{so}^{-1} , however, is small and quite uncertain.

In the region of larger ρ and R values the MR changes character and is not understood. In a first step towards entangling significant sample differences and contradicting theories in this region, the MR was studied in samples prepared by two different techniques; either bars cut from ingots made in an arc furnace or samples made by melt spinning. Although the average temperature dependence of $\rho(T)$ above 4 K is similar for the two sets of samples, there are distinct differences at lower temperatures. The melt-spun samples have a weaker temperature dependence and a smaller MR. We have not been able to correlate these differences to the structure of the samples. This problem must be studied further.

The MR shows qualitative similarities with samples close to the MIT. However, no present theory of the MR on the insulating side could fully reproduce the observations. It is therefore difficult to determine from MR if high resistive *i*-Al-Pd-Re is an insulator.

A major problem is to understand the MR of *i*-Al-Pd-Re in the transition region between QIE and non-QIE behavior [$\rho(4 \text{ K}) \approx 100 \text{ m}\Omega \text{ cm}$]. Determination of τ_{so} may be required. As indicated, results from MR alone do not seem too promising in this respect. Alternative possibilities to obtain τ_{so} must be considered. Measurements of the g factor, and using the relation suggested by Millis and Lee³⁷ could be one possibility to determine F_σ independently, to give improved numerical stability for τ_{so} .

ACKNOWLEDGMENTS

G. Fourcaudot and J. C. Grieco are thanked for their help in preparing the samples, and T. Grenet for many fruitful discussions. Part of this work has been supported by the Swedish Natural Science Research Council, the Göran Gustafsson Foundation, the U.S. National Science Foundation, NSF Grant No. DMR-9700584, and by the French

GdR-CINQ of CNRS. The work has benefitted from exchange research visits between Grenoble and Stockholm, for which the authors gratefully acknowledge support from CNRS (C.B.), and NFR (Ö.R.). One of the authors (M.R.)

gratefully acknowledges the Royal Swedish Academy of Sciences for granting a research visit to LEPES-CNRS, Grenoble, France, and KTH, Stockholm for granting a research period at the University of Virginia, U.S.A.

- ¹Ö. Rapp, in *Physical Properties of Quasicrystals*, edited by Z. M. Stadnik, Springer Series in Solid State Physics Vol. 126 (Springer-Verlag, Berlin, 1999), p. 127ff.
- ²M. Ahlgren, P. Lindqvist, M. Rodmar, and Ö. Rapp, *Phys. Rev. B* **55**, 14 847 (1997).
- ³P. Bancel, *Phys. Rev. Lett.* **63**, 2741 (1989).
- ⁴Y. Honda, K. Edagawa, A. Yoshioka, T. Hasumoto, and S. Takeuchi, *Jpn. J. Appl. Phys., Part 1* **33**, 4929 (1994).
- ⁵S. J. Poon, F. S. Pierce, and Q. Guo, *Phys. Rev. B* **51**, 2777 (1995).
- ⁶C. Gignoux, C. Berger, G. Fourcaudot, J. C. Grieco, and H. Rakoto, *Europhys. Lett.* **39**, 171 (1997).
- ⁷M. Ahlgren, M. Rodmar, J. Brangefält, C. Gignoux, C. Berger, and Ö. Rapp, *Czech. J. Phys.* **46**, 1989 (1996).
- ⁸M. Ahlgren, M. Rodmar, C. Gignoux, C. Berger, and Ö. Rapp, *Mater. Sci. Eng., A* **226-228**, 981 (1997).
- ⁹A. D. Bianchi, F. Bommeli, M. A. Chernikov, U. Gubler, L. Degiorgi, and H. R. Ott, *Phys. Rev. B* **55**, 5730 (1997).
- ¹⁰C. R. Wang, H. S. Kuan, S. T. Lin, and Y. Y. Chen, *J. Phys. Soc. Jpn.* **67**, 2383 (1998).
- ¹¹Q. Guo and S. J. Poon, *Phys. Rev. B* **54**, 12 793 (1996).
- ¹²C. R. Wang, Z. Y. Su, and S. T. Lin, *Solid State Commun.* **108**, 681 (1998).
- ¹³F. S. Pierce, S. J. Poon, and Q. Guo, *Science* **261**, 737 (1993).
- ¹⁴H. Akiyama, Y. Honda, T. Hashimoto, K. Edagawa, and S. Takeuchi, *Jpn. J. Appl. Phys., Part 2* **32**, L1003 (1993).
- ¹⁵S. J. Poon, F. Zavaliche, and C. Beeli, in *Quasicrystals*, edited by J.-M. Dubois, P. A. Thiel, A. P. Tsai, and K. Urban, MRS Symposia Proceedings No. 553 (Materials Research Society, Warrendale, PA, 1999), p. 365.
- ¹⁶J. Delahaye, J. P. Brisson, and C. Berger, *Phys. Rev. Lett.* **81**, 4204 (1998).
- ¹⁷M. Rodmar, F. Zavaliche, S. J. Poon, and Ö. Rapp, *Phys. Rev. B* **60**, 10 807 (1999).
- ¹⁸C. Gignoux, C. Berger, G. Fourcaudot, J. C. Grieco, and F. Cyrot-Lackmann, in *Proceedings of the 5th International Conference on Quasicrystals*, edited by C. Janot and R. Mosseri (World Scientific, Singapore, 1995), p. 452.
- ¹⁹M. Ahlgren, C. Gignoux, M. Rodmar, C. Berger, and Ö. Rapp, *Phys. Rev. B* **55**, R11 915 (1997).
- ²⁰Q. Guo, F. S. Pierce, and S. J. Poon, *Phys. Rev. B* **52**, 3286 (1995).
- ²¹J. Delahaye, C. Gignoux, T. Schaub, C. Berger, T. Grenet, A. Sulpice, J. J. Préjean, and J. C. Lasjaunias, *J. Non-Cryst. Solids* **250-252**, 878 (1999).
- ²²H. Fukuyama and K. Hoshino, *J. Phys. Soc. Jpn.* **50**, 2131 (1981).
- ²³P. A. Lee and T. V. Ramakrishnan, *Phys. Rev. B* **26**, 4009 (1982).
- ²⁴Y. Honda, K. Edagawa, A. Yoshioka, T. Hashimoto, and S. Takeuchi, *Jpn. J. Appl. Phys., Part 1* **33**, 4929 (1994).
- ²⁵F. S. Pierce, Q. Guo, and S. J. Poon, *Phys. Rev. Lett.* **73**, 2220 (1994).
- ²⁶U. Mizutani, *J. Phys.: Condens. Matter* **10**, 4609 (1998).
- ²⁷M. A. Chernikov, A. Bianchi, E. Felder, U. Gubler, and H. R. Ott, *Europhys. Lett.* **35**, 431 (1996).
- ²⁸J. C. Lasjaunias, Y. Calvayrac, and H. S. Yang, *J. Phys. I* **7**, 959 (1997); N. Vernier, G. Bellessa, R. Perrin, A. Zarembovitch, and M. de Boissieu, *Europhys. Lett.* **22**, 187 (1993).
- ²⁹J. J. Préjean, J. C. Lasjaunias, C. Berger, and A. Sulpice (unpublished).
- ³⁰P. Lindqvist, P. Lanco, C. Berger, A. G. M. Jansen, and F. Cyrot-Lackmann, *Phys. Rev. B* **51**, 4796 (1995).
- ³¹H. K. Sin, P. Lindenfeld, and W. L. McLean, *Phys. Rev. B* **30**, 4067 (1984).
- ³²S. Yoshizumi, T. H. Geballe, M. Kunchur, and W. L. McLean, *Phys. Rev. B* **37**, 7094 (1988).
- ³³These exponents arise as follows; in both Eqs. (1) and (2), the expressions for $\Delta\sigma$ are multiplied by $D^{-1/2}$, which roughly gives an additional factor $\rho^{0.5}$ and the traditional value of β of order 1.5. For quasicrystals with large magnetoresistance, one must use $\Delta\sigma(B,T) = -\Delta\rho(B,T)/[\rho(0,T)\rho(B,T)]$ in the conversion from $\Delta\sigma(B,T)$ to $\Delta\rho(B,T)/\rho(0,T)$, and β is then smaller, empirically ≈ 1.3 from Ref. 1.
- ³⁴J. S. Dugdale, *The Electrical Properties of Disordered Metals* (Cambridge University Press, New York, 1995).
- ³⁵M. Matsuo, H. Nakano, S. Saito, M. Mori, and T. Ishimasa, *Solid State Commun.* **86**, 707 (1993).
- ³⁶B. J. Hickey, D. Grieg, and M. A. Howson, *J. Phys.* **16**, L13 (1986).
- ³⁷A. J. Millis and P. A. Lee, *Phys. Rev. B* **30**, 6170 (1984).
- ³⁸A. Sahnoune, J. O. Ström-Olsen, and H. E. Fischer, *Phys. Rev. B* **46**, 10 035 (1992).
- ³⁹M. Paalanen, T. F. Rosenbaum, G. A. Thomas, and R. W. Bhatt, *Phys. Rev. Lett.* **48**, 1284 (1982).
- ⁴⁰G. A. Thomas, M. Paalanen, and T. F. Rosenbaum, *Phys. Rev. B* **27**, 3897 (1983).
- ⁴¹J.-L. Pichard, M. Sanquer, K. Slevin, and P. Debray, *Phys. Rev. Lett.* **65**, 1812 (1990).
- ⁴²Y. Meir, N. S. Wingreen, O. Entin-Wohlman, and B. L. Altshuler, *Phys. Rev. Lett.* **66**, 1517 (1991).
- ⁴³E. Medina, M. Kardar, Y. Shapir, and X. R. Wang, *Phys. Rev. Lett.* **64**, 1816 (1990).
- ⁴⁴E. Medina and M. Kardar, *Phys. Rev. Lett.* **66**, 3187 (1991).
- ⁴⁵M. Eto, *Phys. Rev. B* **51**, 13 066 (1995).
- ⁴⁶Y. Shapir and Z. Ovadyahu, *Phys. Rev. B* **40**, 12 441 (1989).
- ⁴⁷M. Benzaquen, D. Walsh, and K. Mazuruk, *Phys. Rev. B* **38**, 10 933 (1988).
- ⁴⁸H. Fukuyama and K. Yosida, *J. Phys. Soc. Jpn.* **46**, 102 (1979).
- ⁴⁹F. S. Pierce, S. J. Poon, and B. D. Biggs, *Phys. Rev. Lett.* **70**, 3919 (1993).
- ⁵⁰P. A. Lee and T. V. Ramakrishnan, *Rev. Mod. Phys.* **57**, 287 (1985).
- ⁵¹U. Sivan, O. Entin-Wohlman, and Y. Imre, *Phys. Rev. Lett.* **60**, 1566 (1988).

- ⁵²See, e.g., R. Mansfield, in *Hopping Transport*, edited by M. Pollack and B. Shklovskii (North-Holland, Amsterdam, 1991), p. 365.
- ⁵³O. V. Emel'yanenko, D. N. Nasledov, and U. Urmanov, *Fiz. Tekh. Polurovodn.* **2**, 1529 (1968) [*Sov. Phys. Semicond.* **2**, 1275 (1968)].
- ⁵⁴M. Ahlskog, R. Menon, A. J. Heeger, T. Noguchi, and T. Ohnishi, *Phys. Rev. B* **55**, 6777 (1997).
- ⁵⁵B. I. Shklovski and A. L. Efros, in *Electronic Properties of Doped Semiconductors*, edited by M. Cardona (Springer-Verlag, Berlin, 1984), pp. 219–216.